ELSEVIER

Journal of Atmospheric and Solar-Terrestrial Physics 69 (2007) 334–340

Journal of ATMOSPHERIC AND SOLAR-TERRESTRIAL PHYSICS

www.elsevier.com/locate/jastp

Correlation between plasmapause position and solar wind parameters

B.A. Larsen[a,*], D.M. Klumpar[a], C. Gurgiolo[b]

[a]*Space Science and Engineering Laboratory, Department of Physics, Montana State University, Bozeman, MT 59717, USA*
[b]*Bitterroot Basic Research, Hamilton, MT 59840, USA*

Received 17 April 2006; received in revised form 12 June 2006; accepted 14 June 2006
Available online 5 December 2006

Abstract

The average plasmapause radial position is highly dependent on the electric field convection pattern in the inner magnetosphere. We present correlations relating the plasmapause position directly to interplanetary parameters. The plasmapause position is found to be strongly correlated with the interplanetary magnetic field (IMF) B_z component, IMF clock angle, and ϕ, a merging proxy. Delay in the plasmapause response to the arrival of both IMF B_z and IMF clock angle at Earth is found to be 180 min while the delay to the arrival of ϕ is found to be 240 min. A relation is derived between IMF B_z, ϕ, and the plasmapause position. Avoiding the use of geomagnetic indices removes any requirement of knowledge of the current state or response of the magnetosphere.

PACS: 94.30.cv; 94.20.Pp; 94.30.Fk; 96.50.Bh; 94.30.vf

Keywords: Plasmasphere; Plasmapause; Plasma motion; Convection, or circulation in the magnetosphere; Interplanetary magnetic fields; Solar wind/magnetosphere interactions

1. Introduction

The location of the plasmapause is known to vary with geomagnetic activity (Chappell et al., 1970; Carpenter, 1970). Recent work by O'Brien and Moldwin (2003) and Moldwin et al. (2002) has shown correlations between in situ radial plasmapause position determinations and several geomagnetic indices, including K_p, AE, D_{st}, AU, AL, ASY, and ΔD_{st}. They suggest that both convective and substorm electric fields are involved in the determination of plasmapause position due to a stronger correlation between the plasmapause position and AE than with AL or AU. The best model discovered by O'Brien and Moldwin (2003) (as defined by a strong correlation) is based on the minimum D_{st} in the previous 24 h suggesting that D_{st} is a better proxy for the maximum convection electric field strength than is K_p. They also separate out the differences between parameters responsible for fast relative motion of the plasmapause (ΔD_{st}, ASY) and for the absolute plasmapause position (min D_{st}, K_p). The study shows a clear indication of the importance of geomagnetic activity in determining the state of the plasmasphere and the difference in the effectiveness of the various parameters.

*Corresponding author. Tel.: +1 406 994 7321; fax: +1 406 994 4452.
E-mail address: larsen@ssel.montana.edu (B.A. Larsen).

1364-6826/$ - see front matter © 2006 Elsevier Ltd. All rights reserved.
doi:10.1016/j.jastp.2006.06.017

Changes in the strength of the inner magnetospheric convection electric field alter the local particle drift paths which in turn determine the size of the plasmasphere and correspondingly the location of the plasmapause (Kavanagh et al., 1968). Computations of the convection electric field have advanced from the simple uniform convection electric field model of Kavanagh et al. (1968) to the various electric field models based on the Volland–Stern electric field model (Volland, 1978; Stern, 1975). The latter allows inclusion of some shielding effects. The further addition of subauroral polarization streams (SAPS), overshielding, and other localized phenomena (Goldstein et al., 2002, 2003, 2004a) to the field structure has allowed the introduction of localized structure on the average plasmapause.

In this study we explore the correlations of upstream parameters with the average plasmapause position. The parameters explored include the raw ACE measurements together with several derived parameters. These include the IMF magnitude and orientation ($|B|$, $B_{x,y,z}$, δ, λ, $\theta = \arccos(B_z/B_T)$, dB_{rms}), the solar wind velocity, and composition data (V_{sw}, $V_{x,y,z}$, N_{p}, T_{p}, α ratio). Also included are several derived parameters ($P_{\mathrm{dyn}} = N_{\mathrm{p}} V_{\mathrm{sw}}^2$, $E_{kl} = VB_{\mathrm{T}} \sin^2(\theta/2)$, $\phi = VB \sin^2(\theta/2)$). Of these parameters the only ones to show a strong correlation at a particular time delay are the interplanetary magnetic field (IMF) B_z component, the IMF clock angle, and the merging parameter as defined by Kan and Lee (1979). Studying the time delay between changes in interplanetary conditions and any effect that can be seen in the plasmasphere provides not only information on the response or the inertia of the magnetosphere but also possible mechanisms involved in propagating the effects inward. Response times of the plasmasphere to changes in various conditions in the upstream solar wind have been touched on by several authors (Goldstein et al., 2002; Brandt et al., 2002; Goldstein et al., 2005) but never rigorously computed. Using inversions of the EUV plasmaspheric image data we are able to monitor the entire plasmapause for extended periods of time providing excellent statistics. In this initial study we have used an average plasmapause position determined by averaging in magnetic local time (MLT) along the actual boundary. This effectively removed the effects of local plasmapause features such as bite-outs, shoulders, notches, and undulations which have no place in a statistical study of this nature. A study which includes MLT dependence is upcoming. Correlations and time delays between solar wind parameters and plasmapause position (averaged in MLT) provide information both on the overall effect of different upstream parameters on the plasmasphere and how this relates to the magnetosphere as a whole.

2. Data

This study makes use of both the ACE interplanetary field and particle data sets as well the IMAGE EUV plasmaspheric images. The EUV instrument measures the global distribution of He^+ by imaging the resonant scattered emission at 30.4 nm (Sandel et al., 2000). Each image pixel provides the He^+ column density along a line of sight. The images can be inverted to give a mapping of the He^+ density in the SM equatorial plane. The inversion technique is described in detail by Gurgiolo et al. (2005).

The initial step in the inversion process is the removal of background and noise in the measured image. A first estimate is then made of the solution density map and from this a synthetic image is constructed. Comparing the synthetic image to the measured image allows a standard deviation to be computed which provides a measure of the accuracy of the current step in the inversion. A new solution is generated by correcting the previous solution according to the difference seen in the synthetic and measured image pixels. This continues until the synthetic and measured images converge to a minimum standard deviation at which point the inversion is terminated (approximately six iterations).

The plasmapause is then determined from the equatorial density maps derived in the inversion using a semi-automated procedure developed for this study. We have adopted the definition of the plasmapause as the innermost factor of 5 drop in density in less than 0.5 Earth radii (R_{E}) (e.g. Carpenter and Anderson, 1992; O'Brien and Moldwin, 2003), we adopt the same definition in this study. The definition does not handle times when the plasmapause is observed as a gradual decline in density sometimes stretching to geosynchronous orbit. Generally in these cases the location of the plasmapause will be underestimated. Fig. 1 shows an example of the global plasmapause determination from the semi-automated plasmapause locator.

Each plus sign (+) in the figure marks the plasmapause and is obtained by computing the

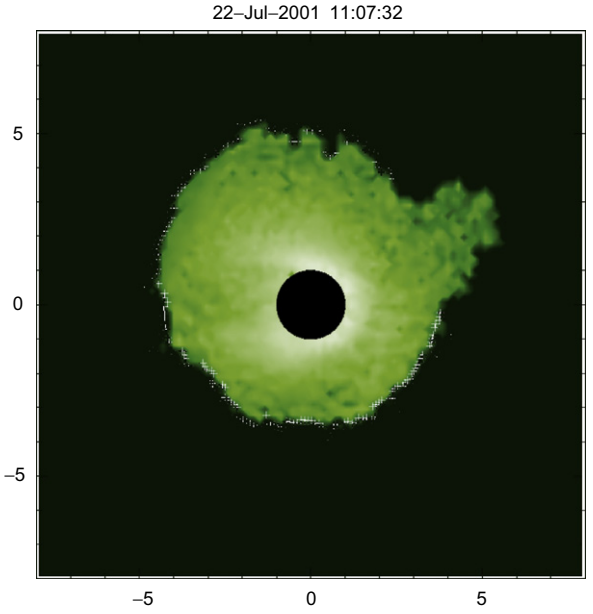

Fig. 1. Example inverted EUV image with the semi-automated extracted plasmapause overplotted. The sun is to the right and the 'bulge'' at about 1300 MLT is an anomaly in the data (light contamination) and therefore does not have plasmapause points for that region.

density gradient along a radial cut and setting the plasmapause at the location which meets the criteria stated above. This removes any subjectiveness from the process of the plasmapause determination which is often present when hand selecting the locations. Each mapping can be quickly scanned for accuracy to be sure that we are not, for example, setting the plasmasphere at the outer edge of a drainage plume (Goldstein and Sandel, 2004b) rather than at the edge of the bulk plasmasphere. Badly determined points are manually deleted from the plasmapause data sets prior to usage.

The base data set used in this study consists of 1365 measured plasmapauses. Fig. 1 is representative of a plasmapause determination. All of the plasmapauses used in this paper come from images taken in 2001. While most consist of full MLT coverage, some have only partial coverage due to data dropouts and light contamination in one of the three IMAGE EUV heads. Averaging over each plasmapause position in a given image (over all MLT) provides a single plasmapause location which is used in the analysis.

Data from the ACE spacecraft (Stone et al., 1998) are used to provide the interplanetary indices used in the correlative study. The data are binned to 10 min averages to match the IMAGE EUV accumulation time. This averaging also acts as a smoothing filter on the interplanetary data. Each 10 min ACE average is time delayed by the measured solar wind speed to the Earth before usage in the correlation analysis.

3. Analysis

The analysis consisted of first identifying a large number of interplanetary parameters and indices which could be either obtained directly or constructed from the ACE data sets and which are candidates to show a correlation with average plasmapause location, L_{pp}. Initial tests showed both the ACE and plasmapause data to be free of significant autocorrelated errors which removed the need to correct for these (Neter et al., 1996). Each of the identified solar wind delayed ACE generated parameters was then correlated with L_{pp} using a nonparametric, rank-order correlation analysis, which made it unnecessary to have any information about the underlying distribution of the data (Press et al., 1992). The Spearman rank-order correlation method was used throughout. The first correlation coefficient is generated using a delay time of −20 min (20 min into the future). Successive coefficients were generated by incrementing the delay time by 5 min at each step, stopping at a delay time of 600 min. Each delay represents a plasmaspheric reaction time. A parameter which is correlated with the average plasmapause location exhibits either a peak or valley in its spectrum at the most probable delay time. A negative time delay (occurrence before the fact) and a zero time delay (instantaneous reaction) are not considered as physical solutions since we assume that there is at least some time delay associated with each response of the system to changes in the external parameters.

The initial set of correlations yielded only three parameters which were found to exhibit a significant correlation peak with L_{pp}. These were the IMF clock angle (θ), IMF B_z component, and the merging proxy, ϕ, defined in Eq. (2). IMF B_z is one of the directly measured ACE products, the IMF clock angle is defined in terms of IMF B_y and B_z as

$$\theta = \arccos\left(\frac{B_z}{\sqrt{B_y^2 + B_z^2}}\right) \quad (1)$$

and ϕ is defined as

$$\phi = vB\sin^2(\theta/2), \quad (2)$$

where v is the solar wind speed, B is the magnitude of the IMF, and θ is the IMF clock angle from Eq. (1).

The correlations for each of the three parameters above is shown in Fig. 2. Also shown is the correlation derived for the solar wind pressure (P_{dyn}). The latter is included to show an example of a parameter showing no correlation peak with L_{pp}.

With the exception of the P_{dyn} correlation in the lower right-hand plot, each plot shows a significant peak or valley in its correlation which occurs at the most probable delay time between the measured parameter arriving at Earth and its affect on the location of the plasmapause. The arrival at Earth is used to avoid ambiguities in the location of the magnetopause. The absence of a peak in the P_{dyn} correlation delay plot indicates that the value of the dynamic pressure has no systematic affect on the plasmapause location. This is not to say that the arrival of interplanetary shocks, high speed streams, and other fast fluctuations of pressure have no effect. They do, but there is no effect for slow changes and near steady state values of the dynamic pressure.

The peaks in the correlated parameters have different widths and positions. The maximum correlation peak in B_z occurs at a delay of 180 min, the θ correlation peak occurs at a delay of 175 min while the ϕ delay is 240 min. The curves relating to B_z and θ are identical within the error bars. (In fact they are essentially identical but mirrored about the Y-axis.) This shows that at the level of precision shown here B_z and θ have the same effect, or more simply only one of them needs to be considered in the end analysis. For the most part we will ignore the θ in the remaining analysis in preference of B_z.

Once the delay times are calculated the next step is to derive expressions which relate the position of the plasmapause as a function of each parameter using the indicated time delay. Using the delay times indicated above (B_z, θ : 180 min, ϕ : 240 min) the linear regression equations are shown in Table 1. The single regression equations yield the following maximum and minimum plasmapause locations for the indicted range of each parameter: $2.99 \rightarrow 4.83$, $3.55 \rightarrow 4.59$, and $2.95 \rightarrow 4.53 R_E$ for B_z, θ, and ϕ, respectively.

Creating one multiple regression equation for the plasmapause from all the parameters (with the appropriate delays for each) yields

$$L_{pp} = 0.050B_{z,180} + 0.108\theta_{175} - 1.110 \times 10^{-4}\phi_{240} + 4.23. \quad (3)$$

The 1σ bootstrap uncertainties computed for the B_z, θ, ϕ slopes, and the intercept are 0.0068, 0.035, 1.59×10^{-5}, and 0.060, respectively. The subscripts on each variable is the delay associated with each parameter. Eq. (3) states that B_z can act to both increase and decrease the average radial position of the plasmapause, θ acts to increase the radial location and then only by a small amount, and ϕ acts to decrease the average radial position. The total change in the plasmapause radial location available from each parameter is 1.47, 0.34, and $0.89 R_E$ for B_z, θ, and ϕ, respectively, showing that the important parameters are B_z and ϕ and not θ. A statistical t-test verifies that the θ coefficient is not statistically different from zero.

Omitting clock angle the multiple regression analysis yields the equation for the plasmapause location below which as expected is almost identical to Eq. (3).

$$L_{pp} = 0.0374B_{z,155} - 1.05 \times 10^{-4}\phi_{275} + 4.38. \quad (4)$$

Fig. 3 is a graphical representation of the data used to derive Eq. (4) with B_z and ϕ varying along the abscissa and ordinate, respectively, and the average radial plasmapause position shown in color. It is easy to see that a large plasmasphere occurs when ϕ is at its lower range with a higher probability when B_z is positive than when it is negative (as might be expected in quiet time conditions).

4. Discussion

Correlation provides a simple means to test for the dependency of one variable on another. In this case, because the correlations are made against time, they also can be used as a predictive tool which allows knowledge of the upstream conditions to be translated with some degree of confidence to conditions at the plasmapause. The large response time in the correlations coupled with the propagation time of the observations at ACE to the Earth allows for L_{pp} to be estimated 3–4 h in the future from real time solar wind measurements.

It is important to remember that the delay times given in a correlation analysis are valid for the 10 min smoothed interplanetary parameters, impulsive events including shocks and IMF turnings

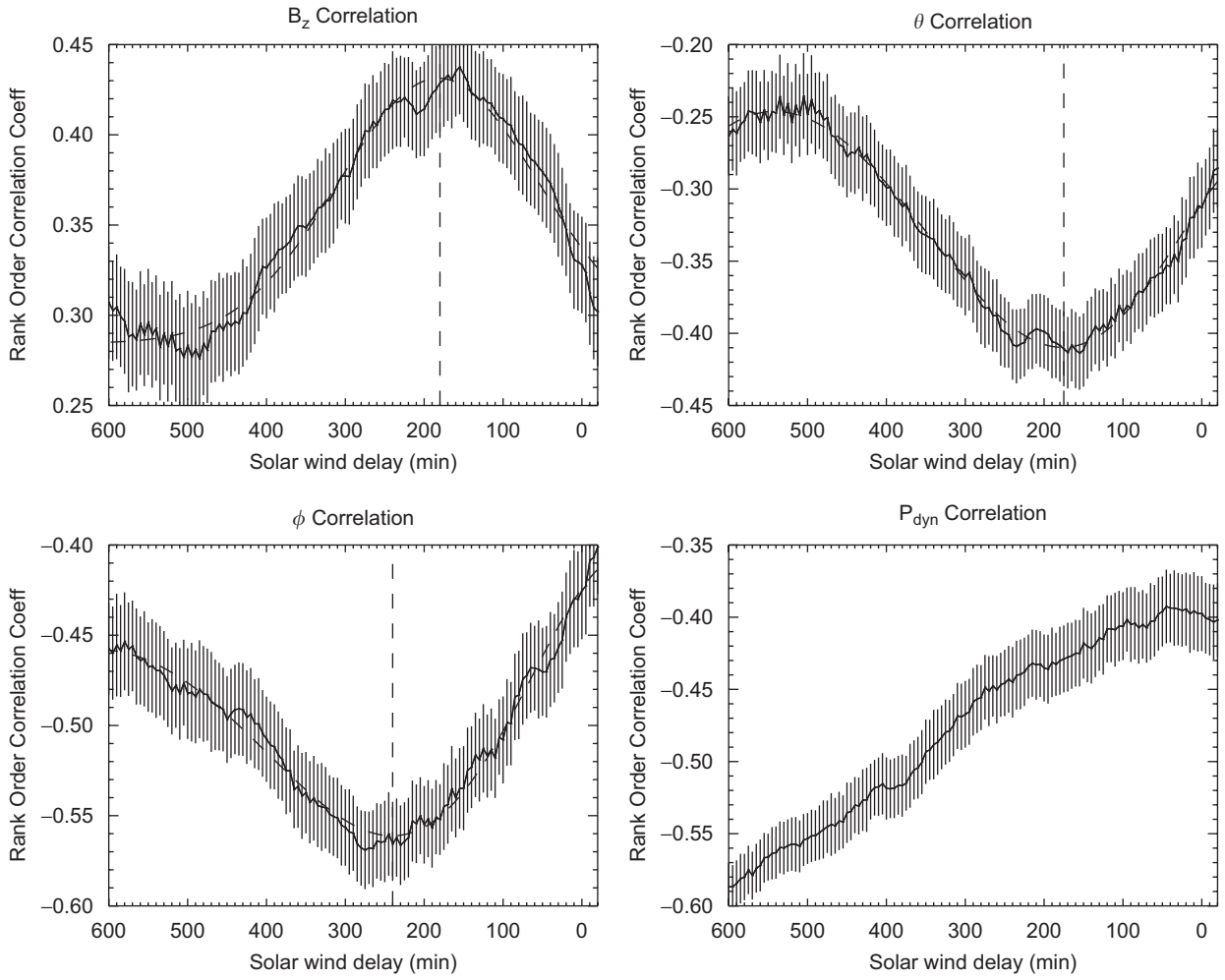

Fig. 2. Rank-order correlation coefficients as a function of solar wind delay (reaction time). The error bars denote 1σ confidence found using bootstrap resampling with replacement. The dashed vertical line denotes the strongest correlation and the dashed lines show a Gaussian fit to the curve used to find the peak.

Table 1
Equations relating plasmasphere position to the three solar wind parameters studied in the paper

Parameter	Slope	Intercept
B_z	$0.062 \pm 0.0027\,\mathrm{nT}R_\mathrm{E}^{-1}$	$4.11 \pm 0.018 R_\mathrm{E}$
θ	$-0.33 \pm 0.021 R_\mathrm{E}^{-1}$	$4.59 \pm 0.040 R_\mathrm{E}$
ϕ	$-1.97 \times 10^{-4} \pm 8.2 \times 10^{-6}\,\mathrm{N\,C^{-1}}\,R_\mathrm{E}^{-1}$	$4.53 \pm 0.022 R_\mathrm{E}$

Parameters studied are IMF B_z, IMF clock angle, θ, and polar cap potential drop, ϕ, as defined in Eq. (2). The uncertainties are 1σ confidence found using bootstrap resampling with replacement.

are not covered in this analysis. We studied the relaxation times of the magnetosphere to a changing input. The system will respond to impulses in any parameter on time scales faster than that produced in the correlations but the time required for the system to reach its final state will be on the time scales similar to those derived in the correlations. As an example, Goldstein et al. (2003) have reported response time of 32 min from the southward turning of B_z to the start of the erosion of the plasmasphere which is considerably more rapid than the 180 min response time predicted in the correlation for B_z. These quick changes in plasmapause position are seen in the statistical study as only starting and ending points of the erosion.

Both B_z and ϕ represent proxies for either conditions or mechanisms in the inner magnetosphere which establish the average radial location of

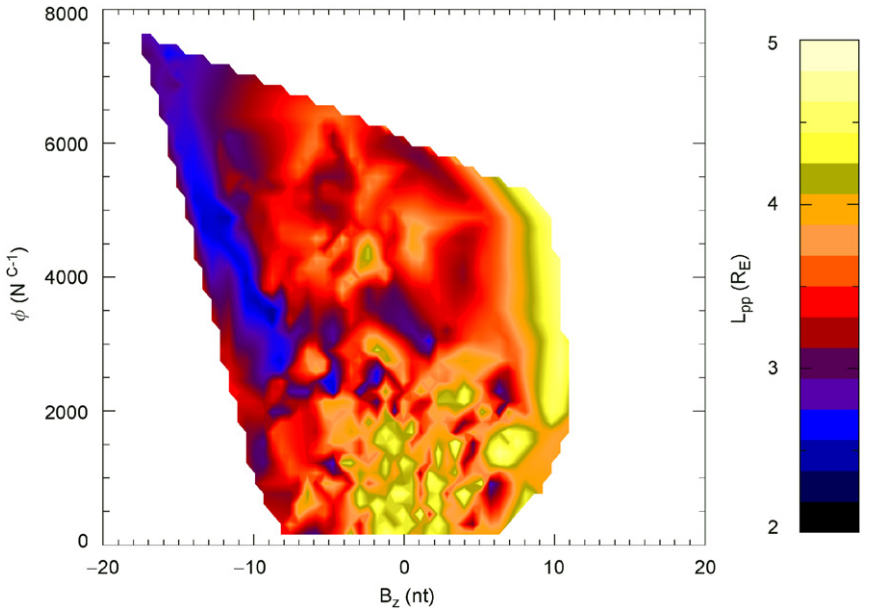

Fig. 3. Contour plot showing the plasmapause reaction to different observed combinations of IMF B_z and the merging proxy, ϕ.

the plasmapause. There is no known direct relationship between the interplanetary conditions and L_{pp}. As such they do not, in themselves, detail how the changes in the L_{pp} occur and must be associated with processes which set up the convection electric field. The key is then to identify the conditions or mechanisms which each proxy represents.

The average plasmapause location is controlled by the combination of the co-rotational and convection electric fields with the convection electric field forming the variable part of the system. It is reasonable to expect then that both B_z and ϕ are proxies for some aspect in the setting up or regulation of the convection field.

It is not surprising that B_z is strongly correlated with L_{pp}. When B_z turns southward, subsolar reconnection becomes possible and the magnetosphere is much more convective thereby increasing the convection electric field. The correlation puts the delay between the arrival of B_z and the new plasmapause position at about 2.5 h.

The correlation of ϕ with L_{pp} is not as obvious as that of B_z. While it contains a dependence on B_z and appears as it should be a reasonable proxy for the interplanetary electric field, it has a significantly longer delay time than associated with B_z which suggests coupling to an additional process. It is reasonable to assume that 3 h of the 4 h response time seen in the correlation is derived from the B_z dependence in the parameter. The source of the remaining hour has yet to be identified but may derive from processes associated with the reconnection of the draped solar wind fields lines in the tail. The 4 h delay time indicated in the correlation is in agreement with the decay times associated with shielding affects mentioned by Dezeeuw et al. (2004), Peymirat et al. (2000), Goldstein et al. (2002).

We can put forth a simple picture of the plasmasphere in which there is a southward turning of the interplanetary field which then remains constant by taking Eq. (4) together with the known plasmaspheric response to impulsive changes in B_z. After approximately 30 min of the interplanetary field turning southward the plasmasphere begins to erode in response to changes in the overall convection field. As the interplanetary conditions steady, the delay between the plasmasphere response to the external changes lengthens to about 3 h. This can be the continuation of the response to the initial turning proceeding at an overall slower pace. Shielding, overshielding, and SAPS which may have been initially set up begin to decay which modifies the convection field and drives the plasmapause at about 4 h from the initial onset, to finally reach its minimum extent. The process reverses when B_z returns northward. Note that in Eq. (4) the expansion of the plasmapause is controlled only by the B_z term.

5. Conclusion

The ability to predict the plasmapause location based solely on upstream parameters is a first step in a predictive model. Using an upstream monitor such as ACE, we can predict the position of the plasmapause at a time in the future determined by the response time as shown in Fig. 2 plus the propagation delay.

Future work will provide the plasmapause location as a function of MLT. Correlations will then show whether the plasmasphere responds as a whole to the changes in the interplanetary conditions or whether different regions respond differently. These future studies, in turn, can be used to provide estimates of the convection electric field which is the ultimate driver of the plasmapause location.

Acknowledgements

B.A. Larsen would like to thank the Montana Space Grant Consortium for its fellowship support, making this work possible. C. Gurgiolo would like to acknowledge support from NASA contract NAS5-96020. We thank the ACE SWEPAM and MAG instrument teams and the ACE Science Center for providing the ACE data. We would like to acknowledge Bill Sandel for many helpful discussions and guidance with the EUV data. The authors would also like to thank the program committee from the 2006 Global Aspects of Magnetosphere–Ionosphere Coupling Yosemite workshop for all their hard work making for an excellent meeting and proceedings.

References

Brandt, P.C., Mitchell, D.G., Ebihara, Y., Sandel, B.R., Roelof, E.C., Burch, J.L., Demajistre, R., 2002. Global IMAGE/HENA observations of the ring current: examples of rapid response to IMF and ring current–plasmasphere interaction. Journal of Geophysical Research 107 (A11), 12.

Carpenter, D.L., 1970. Whistler evidence of the dynamic behavior of the duskside bulge in the plasmasphere. Journal of Geophysical Research 75, 3837–3847.

Carpenter, D.L., Anderson, R.R., 1992. An ISEE/Whistler model of equatorial electron density in the magnetosphere. Journal of Geophysical Research 97 (16), 1097–1108.

Chappell, C.R., Harris, K.K., Sharp, G.W., 1970. The reaction of the plasmapause to varying magnetic activity. In: ASSL vol. 17: Particles and Field in the Magnetosphere, pp. 148–+.

De Zeeuw, D.L., Sazykin, S., Wolf, R.A., Gombosi, T.I., Ridley, A.J., Tóth, G., 2004. Coupling of a global MHD code and an inner magnetospheric model: initial results. Journal of Geophysical Research 109 (A18) A12219.

Goldstein, J., Spiro, R.W., Reiff, P.H., Wolf, R.A., Sandel, B.R., Freeman, J.W., Lambour, R.L., 2002. IMF-driven overshielding electric field and the origin of the plasmaspheric shoulder of May 24, 2000. Geophysical Research Letters 29, 66–1.

Goldstein, J., Sandel, B.R., Hairston, M.R., Reiff, P.H., 2003. Control of plasmaspheric dynamics by both convection and sub-auroral polarization stream. Geophysical Research Letters 30, 6–1.

Goldstein, J., Sandel, B.R., Hairston, M.R., Mende, S.B., 2004a. Plasmapause undulation of 17 April 2002. Geophysical Research Letters 31, L15801.

Goldstein, J., Sandel, B.R., Thomsen, M.F., Spasojević, M., Reiff, P.H., 2004b. Simultaneous remote sensing and in situ observations of plasmaspheric drainage plumes. Journal of Geophysical Research 109 (A18), A3202.

Goldstein, J., Sandel, B.R., Forrester, W.T., Thomsen, M.F., Hairston, M.R., 2005. Global plasmasphere evolution 22–23 April 2001. Journal of Geophysical Research 110 (A9), A12218.

Gurgiolo, C., Sandel, B.R., Perez, J.D., Mitchell, D.G., Pollock, C.J., Larsen, B.A., 2005. Overlap of the plasmasphere and ring current: relation to subauroral ionospheric heating. Journal of Geophysical Research A12217.

Kan, J.R., Lee, L.C., 1979. Energy coupling function and solar wind-magnetosphere dynamo. Geophysical Research Letters 6, 577–580.

Kavanagh, L.D., Freeman, J.W., Chen, A.J., 1968. Plasma flow in the magnetosphere. Journal of Geophysical Research 73 (12), 5511.

Moldwin, M.B., Downward, L., Rassoul, H.K., Amin, R., Anderson, R.R., 2002. A new model of the location of the plasmapause: CRRES results. Journal of Geophysical Research 2.

Neter, J., Kutner, M.H., Nachtsheim, C.J., Wasserman, W., 1996. Applied Linear Statistical Models, fourth ed. Irwin, Chicago.

O'Brien, T.P., Moldwin, M.B., 2003. Empirical plasmapause models from magnetic indices. Geophysical Research Letters 30, 1.

Peymirat, C., Richmond, A.D., Kobea, A.T., 2000. Electrodynamic coupling of high and low latitudes: simulations of shielding/overshielding effects. Journal of Geophysical Research 105, 22991–23004.

Press, W.H., Flannery, B.P., Teukolsky, S.A., Vetterling, W.T., 1992. Numerical Recipes: The Art of Scientific Computing, second ed. Cambridge University Press, Cambridge, UK, New York.

Sandel, B.R., Broadfoot, A.L., Curtis, C.C., King, R.A., Stone, T.C., Hill, R.H., Chen, J., Siegmund, O.H.W., Raffanti, R., Allred, D.D., Turley, R.S., Gallagher, D.L., 2000. The extreme ultraviolet imager investigation for the IMAGE mission. Space Science Reviews 91, 197–242.

Stern, D.P., 1975. The motion of a proton in the equatorial magnetosphere. Journal of Geophysical Research 80, 595–599.

Stone, E.C., Frandsen, A.M., Mewaldt, R.A., Christian, E.R., Margolies, D., Ormes, J.F., Snow, F., 1998. The advanced composition explorer. Space Science Reviews 86, 1–22.

Volland, H., 1978. A model of the magnetospheric electric convection field. Journal of Geophysical Research 83 (12), 2695–2699.